Raman spectroscopy study of the ferrielectric-paraelectric transition in layered CuInP₂S₆

Yu. M. Vysochanskii, V. A. Stephanovich, and A. A. Molnar

Institute for Solid State Physics and Chemistry, Uzhgorod University, Uzhgorod, 29400, Ukraine

V. B. Cajipe* and X. Bourdon

Institut des Matériaux de Nantes, UMR 6502, B.P. 32229, 44322, Nantes, Cedex 3, France

(Received 9 February 1998; revised manuscript received 1 June 1998)

The dynamics of the ferrielectric-paraelectric transition in lamellar CuInP₂S₆ is studied using Raman scattering. Band assignments for this system are established by comparison with published vibrational spectroscopy information on related chalcogenophosphates as well as with new data on SnP₂S₆ herein described. Relaxational rather than resonant behavior is indicated by the temperature dependence of the spectral characteristics, in agreement with the assumed order-disorder character of the transition. It is suggested that a coupling between P₂S₆ deformation modes and Cuᴵ vibrations enables the copper hopping motions which lead to the loss of polarity and the onset of ionic conductivity in this material. [S0163-1829(98)05334-X]

INTRODUCTION

Compounds containing $(P_2X_6)^{4-}$ anions ($X=$S or Se) linked together by metal cations constitute a large family of solids[1–5] which exhibit a variety of interesting physical behaviors. The coordination preferences of different cations are accommodated by the ability of the ethanelike group to withstand variations in P-P and P-X bond lengths, thus leading to three-dimensional (3D) or layered structures. While only a few $M_2P_2X_6$ ($M=$Sn, Pb, Eu, Sr) compounds with a 3D morphology[4] are known to exist, the lamellar chalcogenophosphates are numerous. With heterocharge substitution for divalent M in layered $M_2P_2X_6$ ($M=$Fe, Ni, Mn, Cd, Zn), one can obtain phases such as $A^I B^{III} P_2 X_6$(I-III) and $A^I_{2x} M^{II}_{2-x} P_2 X_6$ (2I-II), in which $A=$Ag, Cu, $B=$V, Cr, In, Sc, and $M=$Mn, Cd, Zn.[1–3] In the layers of these materials, the metal cations and P-P pairs occupy the octahedral voids defined by the chalcogen framework. The A, B, and M of the I-III and $x=1$ 2I-II phases form zigzag chains or triangular motifs within the plane. Introduction of vacant octahedral sites into a layer bearing only one type of cation yields another variation to the layered chalcogenophosphate structure;[6,7] such is the case of $In^{In}_{4/3} P_2 S_6$ and $Sn^{IV} P_2 S_6$.

Recently, we reported ordered dipole arrangements in lamellar $Cu^I B^{III} P_2 S_6$ ($B=$Cr, In).[8–10] The latter is an unusual example of a collinear ferrielectric system and illustrates the general features of cooperative dipole effects within a lamellar chalcogenophosphate. These are quite distinct from those found in 3D $Sn_2P_2S_6$, which undergoes a second-order, displacive paraelectric-ferroelectric transition at 337 K following a continuous thermal evolution of the Sn^{II} position within its sulfur coordination shell.[11] CuInP₂S₆ is ferrielectric at $T < T_c = 315(5)$ K (monoclinic space group C_c) as it contains polar Cu^I and In^{III} sublattices shifted in antiparallel directions relative to the midplane and exhibits a reversible spontaneous polarization $P_s \approx 3$ μC cm⁻² along the perpendicular to the layer. The cation off-centering, 1.6 Å for Cu^I and 0.2 Å for In^{III}, may be attributed to a second-order Jahn-Teller in-

stability associated with the d^{10} electronic configuration.[10] The lamellar matrix absorbs the structural deformations via the flexible P₂S₆ groups while restricting the cations to antiparallel displacements which minimize the energy costs of dipole ordering. In the paraelectric phase (space group $C2/c$), the Cu^I probability density assumes a shape that is twofold symmetric about the center of the octahedral CuS₆ group and elongates along the normal to the layer and into the intermellar space. Earlier Raman spectroscopy[12] and diffraction[10,13] results on $CuBP_2S_6$ ($B=$Cr, In) have pointed to a dynamic interpretation of this disorder. That is, the nonpolar phase is characterized by thermal hopping between the minima of a double-well potential defined by the S₆ cage, and between one such minimum and an interlayer site. The phase transition thus occurs via a cooperative freezing of intersite motions which breaks the twofold symmetry. This transition has been shown to be most probably of the first-order, order-disorder type.[9] At $T \gg T_c$, evidence for ion migration through the lattice has also been found.[14]

In this paper we present Raman scattering data on CuInP₂S₆ recorded at various temperatures as a first approach to studying the dynamics of the ferrielectric-paraelectric transition. We take advantage of the availability of vibrational spectroscopy information on 3D and layered chalcogenophosphates in identifying the observed bands. Within this context, initial Raman measurements on lamellar SnP₂S₆ are also described here. The presentation of the experimental results is followed by a discussion of the symmetry analysis and band assignments for CuInP₂S₆. Finally, the temperature dependence of the Raman spectral characteristics found in this material is interpreted in terms of thermally activated processes responsible for the loss of polar order and the onset of ionic conductivity.

EXPERIMENTAL METHODS

Platelike crystals of CuInP₂S₆, approximately $5 \times 6 \times 0.2$ mm³ in size, were synthesized by solid state reaction as previously described.[9] A similarly prepared $3 \times 2 \times 0.1$ mm³ specimen of SnP₂S₆ was also used. Each
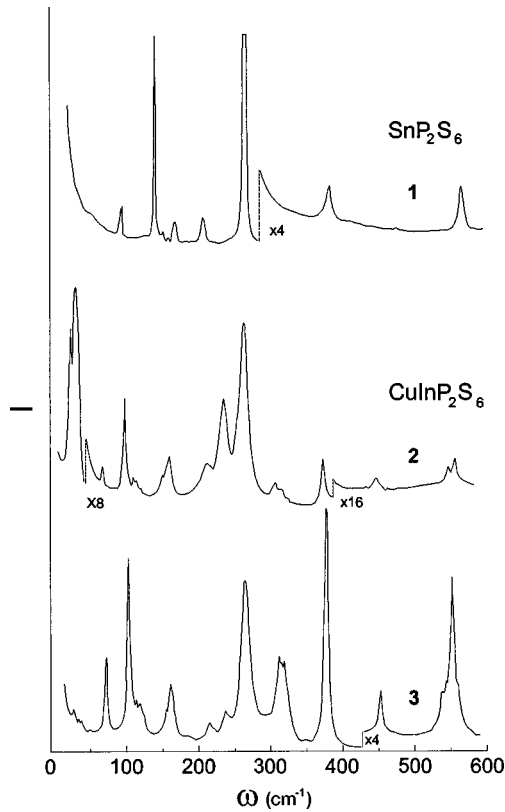
FIG. 1. Raman scattering spectrum for $CuInP_2S_6$ in the $Y(ZY)X$ (bottom) and $Y(ZZ)X$ (middle) geometry and for SnP_2S_6 in the $Y(ZZ)X$ geometry (top).

FIG. 2. Raman scattering spectra for $CuInP_2S_6$ in the $Y(ZZ)X$ geometry at different temperatures: 1, 340 K; 2, 300 K; 3, 250 K; 4, 120 K.

$CuInP_2S_6$ sample was oriented such that the a and b axes coincided with the laboratory X and Y axes, and the normal to the layers (c^*) with the Z axis. For SnP_2S_6, the a and c coincided with the X and Z axes, respectively. The orthogonal $Y(ZZ)X$ light scattering configuration was used in most of the experiments. Polarized radiation from a He-Ne gas laser with a 6328-Å wavelength and power of about 30 mW provided the excitation. The right angle scattering exited across the face of the sample and was analyzed by a DFS-24 two-grating spectrometer with a 2-cm^{-1} spectral resolution. The specimens were loaded under nitrogen vapor in a UTRECS cryostat. The sample temperature was controlled with 0.5 K accuracy. The Raman scattering spectra were normalized relative to the intensity of the band at around 380 cm^{-1} and analyzed via a decomposition into Lorentzian line shapes using the Jandel Scientific Corporation PEAKFIT program. The susceptibilities $\chi''(\omega)$ were determined for a subset of the spectra by taking into account the phonon thermal population.

RESULTS

Polarized Raman spectra for $CuInP_2S_6$ recorded between 5 and 600 cm^{-1} at room temperature in the $Y(ZZ)X$ and $Y(ZY)X$ geometries are displayed in Fig. 1. These spectra should reveal modes of A' and A'' symmetry, respectively (see below). Some overlap of these different symmetry bands, however, occurs because the samples used were quite thin; depolarizing effects due to birefringence and optical activity may likewise be present. For the purposes of this
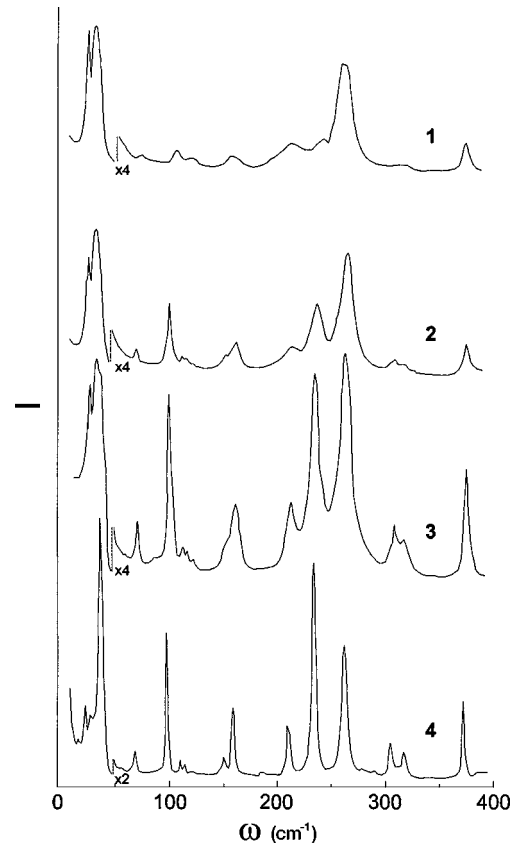
study, it would be sufficient to monitor the thermal evolution of the $Y(ZZ)X$ spectrum (predominantly Z-polarized modes). The cation off-centering responsible for the spontaneous polarization in $CuInP_2S_6$ occurs along the normal to the layers (laboratory Z axis). Moreover, a nondegenerate soft mode, if it exists, should be Raman active and fully symmetric in the polar plane and would be of the type A' in $CuInP_2S_6$. Figure 1 also shows the Raman spectrum for lamellar $Sn^{IV}P_2S_6$ obtained in the $Y(ZZ)X$ geometry (A modes). This will be useful in identifying the bands for $CuInP_2S_6$ as discussed in the next section.

Figure 2 shows a series of spectra measured in the $Y(ZZ)X$ geometry for $CuInP_2S_6$ at various temperatures. Fewer lines can be distinguished in the paraelectric than in the ferrielectric regime, as expected. More striking are thermal changes in the widths and relative intensities found at frequencies below 350 cm^{-1}. Measurements at several temperatures were thus made for two narrower energy windows where the changes are most pronounced: at $190 < \omega < 290$ cm^{-1} and $10 < \omega < 60$ cm^{-1}. Representative spectra are displayed in Figs. 3 and 4. The susceptibility $\chi''(\omega)$ was calculated for the spectra in the latter energy range to better depict the relative contributions of the low-energy phonons (Fig. 4, right). Lorentzian line shape fits were performed on the complete data set. The evolution of the spectral features is summarized by plotting selected fit parameters versus temperature (Fig. 5).

In the higher-frequency range, the half widths at half maximum of the bands at 240 and 280 cm^{-1} exhibit an
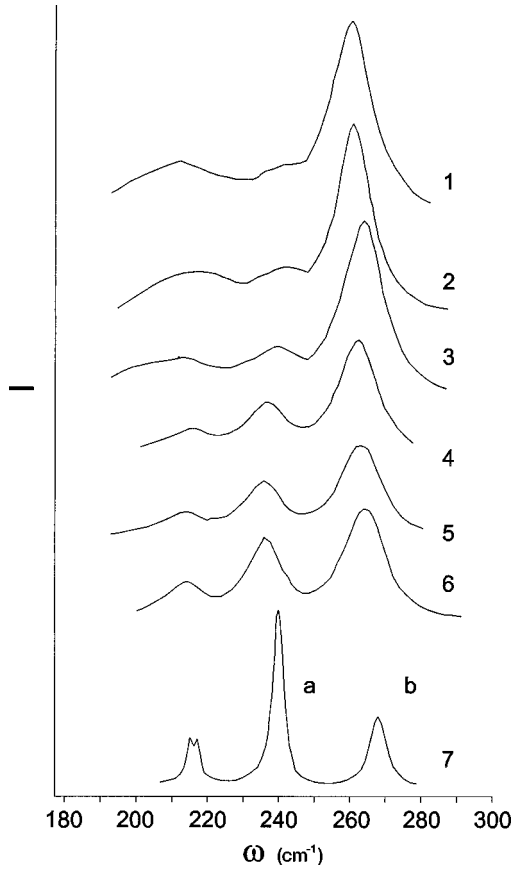
FIG. 3. Spectral lines within the energy range of P_2S_6 deformation modes in $CuInP_2S_6$ at various temperatures: 1, 370 K; 2, 329 K; 3, 319 K; 4, 311 K; 5, 306 K; 6, 299 K; 7, 95 K.

FIG. 4. Low-frequency cation vibrational bands in $CuInP_2S_6$ at different temperatures: 1, 370 K; 2, 329 K; 3, 321 K; 4, 319 K, 5, 316 K; 6, 311 K; 7, 306 K; 8, 299 K; 9, 95 K. The corresponding susceptibility curves $\chi''(\omega)$ are also shown.

anomalous change within the 305–325 K interval. In particular, the half width of the 240-cm^{-1} peak increases smoothly from approximately 3 cm^{-1} at 95 K to 10 cm^{-1} at 300 K, then rapidly to 13 cm^{-1} just above 320 K, beyond which the thermal change is less significant. Similar behavior is observed in the temperature dependence of the relative intensities of these two bands. In the low-energy range, peaks at 28, 33, and 43 cm^{-1} are clearly observed at 95 K (Figs. 4 and 5). The highest-energy band of this group shifts down to 34 cm^{-1} upon warming to 300 K, then to higher wave numbers up to 330 K and back towards lower energies with further heating. Anomalous decreases in the wave numbers of the other two low-energy modes are likewise observed at $305 < T < 325$ K, but in no case is a shift to zero frequency found. A marked intensity redistribution among the three low-energy bands occurs as T is increased. Specifically, the intensities of the two lower-energy lines grow at the expense of that at higher energy. A very weak band close to 22 cm^{-1} also appears at $T > 310$ K (Fig. 4). The above observations are consistent with the occurrence of a first-order phase transition in $CuInP_2S_6$ between 305 and 325 K.

SYMMETRY ANALYSIS AND BAND ASSIGNMENTS

The symmetry analysis of the vibrational modes of $CuInP_2S_6$ follows from correlating the symmetry group of the $(P_2S_6)^{4-}$ anions and those of the cation sites with the point group of the crystal. Free $(P_2S_6)^{4-}$ anions have D_{3d}
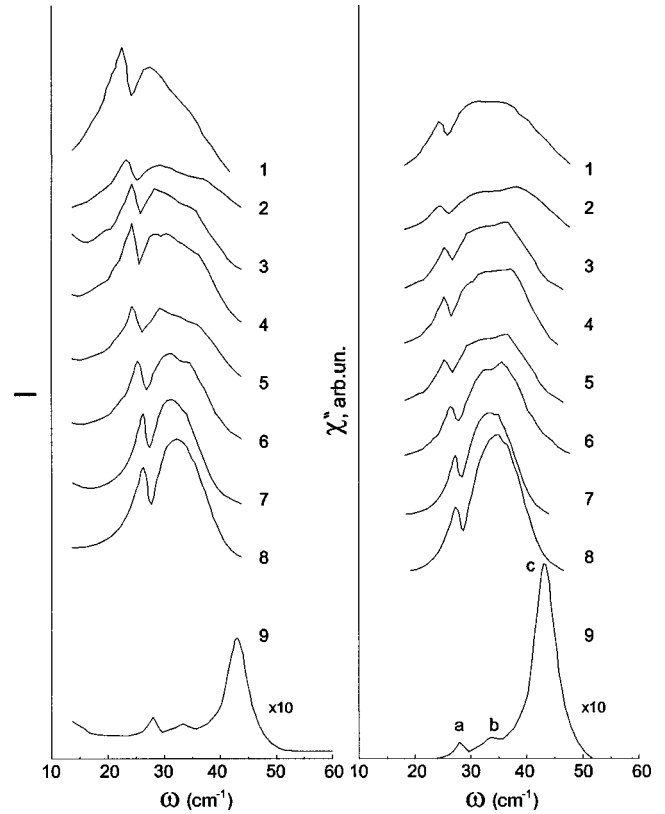
symmetry and exhibit the following internal modes:[15]

$$\Gamma_{int}(P_2S_6) = 3A_{1g}(R) + A_{1u} + 2A_{2u}(IR) + 3E_g(R)$$
$$+ 3E_u(IR),$$

where R and IR designate the Raman- and infrared-active modes, respectively. The internal vibrations may be divided into four groups, which will be referred to as the P-S, P-P, S-P-S, and S-P-P modes. Four P-S bond stretching vibrations (ν) account for $A_{1g} + A_{2u} + E_u + E_g$. The antiphase motions of the PS_3 groups stretch the P-P bond and have A_{1g} symmetry. S-P-S deformation modes (δ) which change the S-P-S angles give another set of $A_{1g} + A_{2u} + E_u + E_g$. The S-P-P bending vibrations, i.e., the bending of the PS_3 groups relative to the P-P bond, account for $E_u + E_g$. The A_{1u} mode corresponds to a twisting $(P_2S_6)^{4-}$ oscillation.

The structure of $CuInP_2S_6$ in the ferrielectric phase (space group Cc, point group m) (Refs. 9 and 10) is described with four formula units in the unit cell and all atoms in general positions (C_1). The primitive cell contains two formula units within a single layer. The irreducible representations of the optical and acoustic vibrations are

$$\Gamma_{opt} = 28A' + 29A'', \quad \Gamma_{acoust} = 2A' + A'',$$

where both A' and A'' are Raman and infrared active. Here the internal $(P_2S_6)^{4-}$ modes split into $36A$ vibrations via a resonance interaction between two anions per primitive cell. The external translations and librations of the anions account
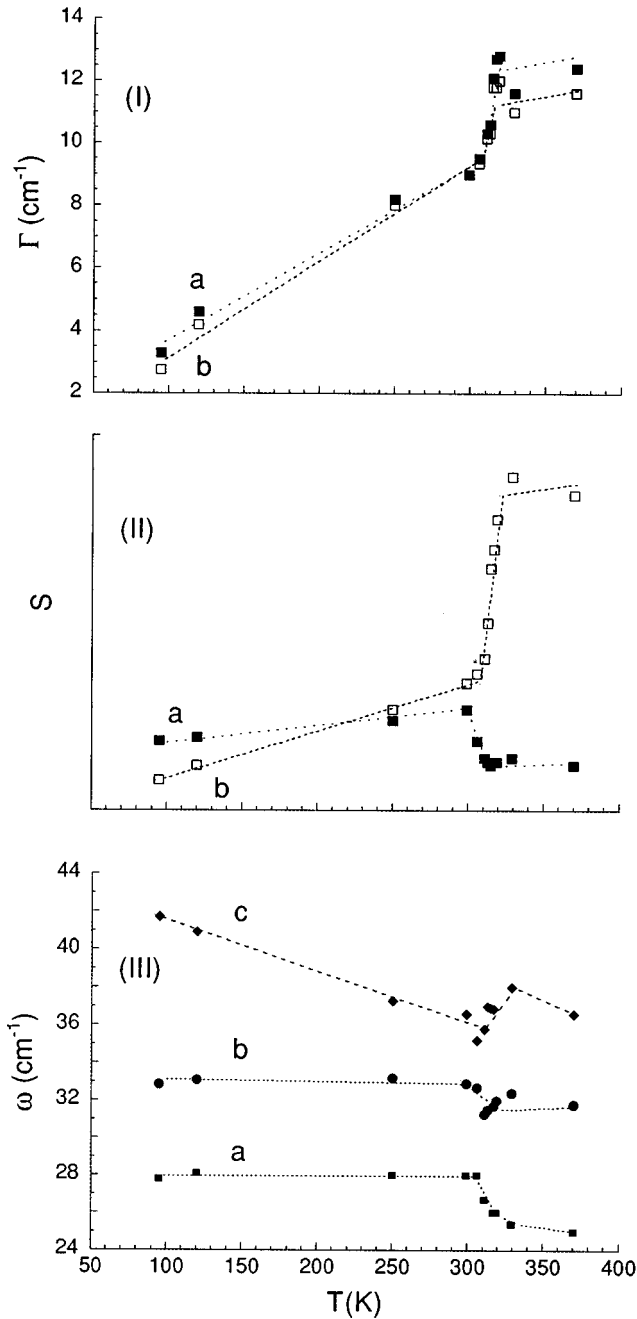
FIG. 5. Temperature dependence of the peak width or damping (I) and integrated intensity (II) of spectral lines marked *a* and *b* in Fig. 3 and of the band frequency (III) of phonons marked *a*, *b*, and *c* in Fig. 4.

for $12A$ modes, the remaining modes being attributable to cation motions. In the paraelectric phase (space group $C2/c$, point group $2/m$),[10] the primitive cell still contains two formula units. Cu and In are found in twofold-symmetric sites (C_2), while P and S occupy general positions. The expected modes are

$$\Gamma_{opt} = 14A_g(R) + 16B_g(R) + 13A_u(IR) + 14B_u(IR),$$

$$\Gamma_{acoust} = A_u + 2B_u.$$

The internal $(P_2S_6)^{4-}$ vibrations are given by $9A_g + 9B_g + 9A_u + 9B_u$. There are 21 external optical modes of which $2A_g + 4B_g + 2A_u + 4B_u$ are due to cation translations.

The room temperature structure of $Sn^{IV}P_2S_6$ has been described within the noncentrosymmetric group $R3$ with all atoms in C_3 sites.[7] The rhombohedral primitive cell contains only one $(P_2S_6)^{4-}$ and one cation, and so the modes are

$$\Gamma_{opt} = 8A + 8E, \quad \Gamma_{acoust} = A + E,$$

where both A and E are Raman and infrared active. The internal anion modes are given by $\Gamma_{int}(P_2S_6) = 6A + 6E$. Of the $3A + 3E$ external modes, only $2A + 2E$ are optical.

$CuInP_2S_6$ and $Sn^{IV}P_2S_6$ represent the extrema of the degree to which the $(P_2X_6)^{4-}$ anion is described by the crystal field within the chalcogenophosphate series $A^IB^{III}P_2X_6 - M_2^{II}P_2X_6 - M^{IV}P_2X_6$. Splitting of the internal anion modes would be significant in the presence of two cation types, and least in SnP_2S_6. The next most symmetric case is that of layered $Fe_2P_2Se_6$, which has $(P_2Se_6)^{4-}$ in a C_3 site and one formula unit per primitive cell, followed by $Fe_2P_2S_6$ with $(P_2S_6)^{4-}$ occupying a C_{2h} site.[16] Towards the other extreme, the 3D compound $Sn_2^{II}P_2S_6$ in the paraelectric phase (space group $P2_1/c$) has a primitive cell with two formula units and $(P_2S_6)^{4-}$ in C_i sites;[11] the internal anion modes are the same as in paraelectric $CuInP_2S_6$. The external lattice vibrations evolve likewise across the chalcogenophosphate series: SnP_2S_6 has 4 optic external optic modes, while both paraelectric $Sn_2P_2S_6$ and $CuInP_2S_6$ have 21.

Detailed polarized Raman spectroscopy studies[11] have been conducted on $Sn_2^{II}P_2S_6$. The internal anion vibration therein are known to occur between 160 and 600 cm^{-1}. The P-S valence vibrations appear in the 550–600 cm^{-1} interval, the P-P stretching around 380 cm^{-1}, the S-P-S deformations in the 190–260 cm^{-1} region, and the S-P-P bending motions near 170 cm^{-1}. Internal modes of the same symmetry may couple so that P-P (P-S) modes may contribute to the 550–600 cm^{-1} (380 cm^{-1}) bands, for example.[12] The external modes occur below 150 cm^{-1}, the anion librations appearing between 85 and 150 cm^{-1} and the cation translations between 26 and 70 cm^{-1}. For the layered thiophosphates[12,16–18] the internal and external modes are located in wave number ranges analogous to those in 3D $Sn_2P_2S_6$. Since the $(P_2S_6)^{4-}$ group has more open basal triangles and a variety of possible cation environments in the lamellar structure, the coupling of same symmetry modes therein would differ from those in the 3D case.

Not at all of the $28A' + 29A''$ Raman modes expected in ferrielectric $CuInP_2S_6$ were observed. Twenty bands are found in the $Y(ZZ)X$ spectrum and 21 in the $Y(ZY)X$ (Fig. 1), some of which may be depolarized. It may be supposed that the most intense of these correspond to the $14A_g + 16B_g$ of the paraelectric phase, the weaker bands originating from the $13A_u(IR) + 14B_u(IR)$. Similar effects[11] have been found in the case of $Sn_2^{II}P_2S_6$. The weak Raman activity of the A' bands deriving from A_u and B_u models is also consistent with the relatively small spontaneous polarization in ferrielectric $CuInP_2S_6$. The $Y(ZZ)X$ spectrum of SnP_2S_6 contains 11 bands, i.e., more than the $8A$ predicted by symmetry analysis. The extra lines are most probably depolarized E modes.

Despite the ambiguity imposed by the mentioned depolarizing effects, band assignments may be established by cross-referencing within the chalcogenophosphate family. For both

compounds studied here, the lines between 140 and 570 cm^{-1} may be ascribed to internal anion vibrations and those at lower wave numbers to external modes. The $6A$ internal $(P_2S_6)^{4-}$ vibrations in SnP_2S_6 would then be the coupled ν(P-S) and ν(P-P) at 566 and 380 cm^{-1}, the δ(S-P-S) at 173, 209, and 266 cm^{-1}, and the δ(S-P-P) at 144 cm^{-1}; the line at 100 cm^{-1} is most probably due to anion librations and the weak band at 57 cm^{-1} to Sn^{IV} translations. Analogous assignments may be made for the richer spectral features of $CuInP_2S_6$, with the δ(S-P-P) and δ(S-P-S) modes appearing at $140 < \omega < 340$ cm^{-1}. The new bands between 300 and 320 cm^{-1} and the multiple peaks in the 90–120 cm^{-1} (mostly anion librations) and 20–70 cm^{-1} (cation translations) ranges arise in the presence of two cation types. This has likewise been noticed in $Cu_{2x}^I M_{2-x}^{II} P_2S_6$ ($M=$ Mn, Cd) (Ref. 18) where Cu^I–Cu^I pairs randomly substitute for M^{II}. In these I-II compounds, greater copper content leads to an intensity increase for the 300–320 cm^{-1} modes and a decrease for the band at 270 cm^{-1}. These anion deformation modes are thus closely related to distortions within the S_6 cage occupied by Cu^I. The lowest-frequency bands contain relative translations T' of the Cu^I, In^{III}, and the center of mass of the P_2S_6 anion, but it may be supposed that cation contributions dominate. Based on a comparison of Raman spectra for $M_2P_2S_6$ and $Cu_{2x}^I M_{2-x}^{II} P_2S_6$ ($M=$ Mn, Cd), the modes due to Cu^I in the latter were determined to appear at wave numbers lower than those for the M^{II} modes. Assuming that the same relationship holds for cation modes in $CuInP_2S_6$, the bands below (above) 50 cm^{-1} may be assigned to Cu^I (In^{III}). A mixed cation character for these lines may, however, not be precluded.

DISCUSSION

It is clear from the preceding section that the thermal evolution observed in the $Y(ZZ)X$ spectra of $CuInP_2S_6$ primarily involves cation translation and P_2S_6 deformation modes. None of the low-frequency cation vibrations merges with the excitation line as T approaches T_c; i.e., the phase transition is not brought about by the condensation of a soft phonon. This is consistent not only with the expectation of an order-disorder rather than a displacive-type transition, but also with the absence of tunneling with the supposed double-well potential.[19] As deduced from crystallographic results on $CuBP_2S_6$ ($B=$ Cr, In), the transition in these materials is triggered by an ordering of the Cu^I sublattice. In $CuInP_2S_6$, it then appears that T-dependent positional shifts[10] of In^{III} do not constitute a displacive component and the transition dynamics would be relaxational. The changes in wave number and relative intensities of the low-frequency bands might be explained by a coupling between quasiharmonic oscillators, i.e., the phonon at 28 and 33 cm^{-1} interacting with that at 43 cm^{-1}. A more intuitive explanation of the low-frequency behavior may, however, be given in terms of thermally activated cation motions. This latter appears plausible considering that the P_2S_6 deformation modes likewise undergo thermal changes.

In $Cu_{2x}Mn_{2-x}P_2S_6$, an intensity redistribution among the low-frequency Raman bands was also observed upon heating.[18] This was modeled by assuming a thermally activated process mediated by a nonlinear coupling between a lattice vibration and the Cu^I translational mode normal to the layer. Specifically, it was suggested that populating the excited states for the P_2S_6 deformation modes enables a Cu^I to pass through the basal triangle of a S_6 cage and into the interlayer gap. With the bands at 60 and 45 cm^{-1} assigned to T'_z vibrations of Cu^I within an intralayer and interlayer site, respectively, changes in the relative intensities would correspond to a T-enhanced occupation of the latter. Because no simultaneous thermal evolution was detected in the 250–350 cm^{-1} range, it was supposed that the copper T'_z potential does not change significantly with warming.

The case of $CuInP_2S_6$ is related, but different. In the average structure, the Cu^I ions do not exist as ''static'' bimetallic pairs as in $Cu_{2x}Mn_{2-x}P_2S_6$, but singly occupy an S_6 unit. Crystallographic results have shown that some copper hopping motions may already occur at 153 K $< T < T_c$ between the off-center intralayer site and its twofold equivalent, as well as between the intra- and interlayer sites. At $T > T_c$, the copper ions assume a twofold-symmetric distribution over the various possible sites. There are thus two thermally activated processes here, one which is responsible for the loss of polarity and the other which intensifies in the nonpolar phase and precedes ionic conductivity.[14] An interdependence may be assumed between the excited states of the P_2S_6 modes and the occurrence of both types of intersite hopping. Structural data give an indication of this.[10] With the Cu^I in the upper off-center minimum of the double-well potential, the PS$_3$ groups undergo clockwise twists associated with the slight downward off-centering of the P-P pair and the longer (shorter) P-S distances and smaller (bigger), less (more) dispersed S-P-S angles in the upper (lower) PS$_3$ group. The S-P-P angles are also larger and more disparate in the upper than the lower pyramid. Up and down flipping of the Cu^I dipole would then be accompanied by reversals of these P_2S_6 strains. Furthermore, the dispersion in P-S bond lengths was found to be greater in the paraelectric than in the ferrielectric phase and much more so when a partial occupation could be refined for the interlayer site.

A reasonable interpretation of the T dependence observed in Figs. 3–5 may be given by ascribing the low-frequency bands to Cu^I translations. The line at 43 cm^{-1} in the 95-K spectrum would be due to T'_z vibrations in the favored, upper off-center site within the layer. Those at lower frequencies most probably represent T'_z vibrations in other copper sites or T'_{x-y} modes. The ''softening'' of the 43-cm^{-1} line within the ferrielectric regime reflects the anharmonicity of the potential around the upper off-center site which allows minority occupation of the lower off-center site and some jumping out of the layer. The intensity redistribution among the low-frequency lines and between the P_2S_6 deformation bands at $220 < \omega < 280$ cm^{-1}, as well as the damping of the latter at $T < T_c$, may likewise be related to Cu^I hopping motions in the polar phase. All anomalous changes observed between 305 and 325 K (Fig. 5) certainly have to do with the recovery of twofold symmetry via double-well hopping; this then feeds jumps into the interlayer gap to the extent that the excited states of the relevant P_2S_6 deformation modes are populated. Shifts in the Cu^I translation mode frequencies at $305 < T < 325$ K indicate modifications in the shape of the ion potential upon crossing the transition. The potential is

defined by the sulfur environment, which in turn is determined by the P_2S_6 state at a given T. Relative intensities in the low-frequency spectrum then evolve according to the T-dependent occupancies of the potential minima. Last, it is worth noting that the nondetection of thermal changes in the P_2S_6 deformation bands in $Cu_{2x}Mn_{2-x}P_2S_6$ confirms that those observed here are related to the loss of polarity.

The mean amplitude of the cation vibrations in the Z direction (c^* axis) may be evaluated from the U_{33} component of the thermal factor obtained in the crystallographic study.[10] At 153 K, $\langle u_z^2 \rangle^{1/2}$ is 0.22 Å for Cu^I in the off-center intralayer site and 0.10 Å for In^{III}; these rise to 0.35 and 0.14 Å, respectively, at room temperature. The mean amplitude may also be estimated in the harmonic approximation from the T_z' frequency via the Cruickshank equation.[18] Thus, for the band appearing at 40 cm^{-1} at 153 K and 35 cm^{-1} at 300 K, one gets 0.19 and 0.31 Å, respectively. These values compare quite well with the those given by crystallography for off-center Cu^I. The interpretation proposed above for the T dependence of the Raman spectra is also consistent with recent neutron scattering results[20] on $CuInP_2S_6$. Quasielastic scattering indicative of hopping motions was observed at $T > T_c$ and disappeared only well below the transition. Moreover, an inelastic peak which conceivably represents more than one optical phonon was detected around 3.7 meV (≈ 30 cm^{-1}). Because the neutron scattering cross section for indium is relatively insignificant, these features are most likely attributable to copper ion dynamics.

In closing, the results of the present work indicate a re-laxational rather than resonant response for $CuInP_2S_6$ and agree with the hypothesis of dynamic disorder in the paraelectric phase. The evolution with temperature of the $Y(ZZ)X$ Raman spectra could be explained in terms of thermally activated processes by a coupling between P_2S_6 deformation modes and Cu^I vibrations; these then effect the occurrence of the transition and ion transport in this system. Dielectric measurements are currently being carried out to further characterize these polarization mechanisms. A modeling of the lattice dynamics is also envisioned to confirm the assumed interaction between anion and cation modes. It is clear that a comprehensive polarized Raman spectroscopy study which allows identification of all theoretically predicted vibrations would be essential to a more quantitative description of the transition dynamics. We are currently trying to prepare thicker samples which should make such an investigation possible. Other work in progress includes NMR spectroscopy experiments, total-energy pseudopotential calculations, and the detailed analysis of neutron scattering data on $CuInP_2S_6$.

*Author to whom correspondence should be addressed. FAX: 33 2 40 37 39 95. Electronic address: cajipe@000cnrs-imn.fr

[1] W. Klingen, G. Eulenberger, and H. Hahn, Z. Anorg. Allg. Chem. **401**, 97 (1973); R. Brec, Solid State Ionics **22**, 3 (1986); S. Lee, J. Am. Chem. Soc. **110**, 8000 (1988).

[2] Y. Mathey, A. Michalowicz, P. Toffoli, and G. Vlaic, Inorg. Chem. **23**, 897 (1984).

[3] R. Pfeiff and R. Kniep, J. Alloys Compd. **186**, 111 (1992).

[4] C. D. Carpentier and R. Nitsche, Mater. Res. Bull. **9**, 401 (1974); **9**, 1097 (1974).

[5] Yu. M. Vysochanskii and V. Yu. Slivka, Sov. Phys. Usp. **35**, 123 (1992).

[6] R. Diehl and C. D. Carpentier, Acta Crystallogr., Sect. B: Struct. Crystallogr. Cryst. Chem. **34**, 1097 (1978).

[7] Z. Wang, R. D. Willett, R. A. Laitinen, and D. A. Cleary, Chem. Mater. **7**, 856 (1995).

[8] V. Maisonneuve, V. B. Cajipe, and C. Payen, Chem. Mater. **5**, 758 (1993).

[9] V. Maissonneuve, M. Evain, C. Payen, V. B. Cajipe, and P. Moliniée, J. Alloys Compd. **218**, 157 (1995); A. Simon, J. Ravez, V. Maisonneuve, C. Payen, and V. B. Cajipe, Chem. Mater. **6**, 1575 (1994).

[10] V. Maissonneuve, V. B. Cajipe, A. Simon, R. von der Muhll, and J. Ravez, Phys. Rev. B **56**, 10 860 (1997).

[11] Yu. M. Vysochanskii, Yu. V. Voroshilov, M. I. Gurzan, and D. V. Chepur, Fiz. Tverd. Tela (Leningrad) **21**, 211 (1979) [Sov. Phys. Solid State **21**, 123 (1979)]; **21**, 2402 (1979) [Sov. Phys. Solid State **21**, 1382 (1979)]; A. V. Gomonnai, Yu. M. Vysoch-anskii, A. A. Grabar, and V. Yu. Slivka, *ibid.* **23**, 3623 (1981) [*ibid.* **23**, 2105 (1981)].

[12] C. Payen, P. McMillan, and P. Colombet, Eur. J. Solid State Inorg. Chem. **27**, 881 (1990).

[13] V. Maisonneuve, C. Payen, and V. B. Cajipe, J. Solid State Chem. **116**, 208 (1995).

[14] V. Maissonneuve, J. M. Réau, M. Dong, V. B. Cajipe, C. Payen, and J. Ravez, Ferroelectrics **196**, 257 (1997).

[15] G. Herzberg, *Infrared and Raman Spectra of Polyatomic Molecules*, 3rd ed. (Van Nostrand, New York, 1947).

[16] G. Kliche, J. Solid State Chem. **51**, 118 (1984); M. Scagliotti, M. Jouanne, M. Balkanski, G. Ouvrard, and G. Benedek, Phys. Rev. B **35**, 7097 (1987).

[17] Von H. Burger and H. Falius, Z. Anorg. Allg. Chem. **363**, 24 (1968); W. Klingen, R. Ott, and H. Hahn, *ibid.* **396**, 271 (1973); Y. Mathey, R. Clement, C. Surisseau, and G. Lucazeau, Inorg. Chem. **19**, 2773 (1980); R. Mercier, J. P. Malugani, B. Fahus, J. Douglade, and G. Robert, J. Solid State Chem. **43**, 151 (1982); C. Sourisseau, J. P. Forgerit, and Y. Mathey, *ibid.* **49**, 134 (1983); W. Brockner and U. Patzmann, Z. Naturforsch. A **38**, 92 (1983).

[18] Y. Mathey, R. Clement, J. P. Audiere, O. Poizat, and C. Sourisseau, Solid State Ionics **9&10**, 459 (1983); O. Poizat, C. Sourisseau, and Y. Mathey, J. Solid State Chem. **72**, 272 (1988); O. Poizat, F. Fillaux, and C. Sourisseau, *ibid.* **72**, 283 (1988).

[19] R. Blinc and B. Zeks, *Soft Modes in Ferroelectrics and Antiferroelectrics* (North-Holland, Amsterdam, 1974), p. 15.

[20] V. B. Cajipe, C. Payen, H. Mutka, and H. Schrober (unpublished).